

Application of Nonlinear Control to a HAWT

D.J.Leith
W.E. Leithead

Department of Electronic & Electrical Engineering,
University of Strathclyde
GLASGOW G1 1QE, U.K.

Abstract

Wind energy is one of the most promising sources of renewable energy for the UK. Over the last two decades there has been rapid development of the technology, and in the UK several commercial wind farms are in operation with more under construction. The standard commercial design of wind turbine is a horizontal axis grid-connected up-wind machine with a rating of approximately 300 kW. The rotor usually has two or three blades, and in pitch regulated machines the pitch angle of either the full span of the blades or just the outer tips can be varied. The application of a nonlinear controller to a typical two-bladed machine with full-span pitch control is investigated in the present paper. It is known that this particular configuration of wind turbine presents a more demanding control problem than alternative configurations, and the benefits of a more sophisticated control system are therefore expected to be greater in the two-bladed case.

Introduction

As the wind is turbulent, it is a stochastic source of energy. Accordingly, the power generated by the turbine and the loads on the turbine vary rapidly in a random manner; for example, the level of generated power may change by 50% in one or two seconds. The aim of the control system is to vary the blade pitch angle to meet the following general objectives :

- to alleviate stress throughout the wind turbine
- to smooth power
- to maximise energy capture

The control system is also required of course to induce appropriate dynamic characteristics in the drive-train of the wind turbine. The controller is only active above the wind speed, rated wind speed, at which the rated power of the turbine is attained, i.e. 300 kW in the turbine considered here.

The actuator characteristics, especially the limits on its torque, impose the main restriction on the performance that can be achieved by a controller. In the case of a wind turbine, as wind speed rises a linear controller places less demand on the actuator since the sensitivity of the aerodynamic torque to pitch changes increases faster than the sensitivity to wind speed changes. Hence, for a controller with fixed open-loop cross-over frequency while the actuator may be worked to its full capacity at low wind speeds, it may not be used as fully at

higher wind speeds. However, it is at these higher wind speeds that the loads are highest, and therefore controller performance is most critical. Theoretical studies [1] predict that there is an advantage in using this spare actuator capacity to enable an increased open-loop cross-over frequency to be realised as the wind speed rises; that is, a suitable nonlinear controller may lead to improved performance. However, there are two competing requirements as explained below. As wind speed rises, for a fixed controller the standard deviation of the power output also rises due to the increased level of turbulence. It is therefore attractive to increase the open-loop cross-over frequency, giving improved disturbance rejection. However, the wind experienced by a wind turbine contains large amounts of energy at frequencies corresponding to multiples of the rotational speed of the rotor, P , and so the wind speed spectrum differs from that experienced at a static point (see e.g. [3]). A typical wind spectrum for a two-bladed machine is shown in figure 1. The large peaks are evident at $2P$ and $4P$. Since it is necessary to protect the actuator by causing the open-loop transmittance to roll-off whilst maintaining adequate gain and phase margins, there is an inevitable tendency for the sensitivity function to increase the intensity of the $2P$ and $4P$ peaks as the cross-over frequency is increased. The result is that there exists an optimum cross-over frequency for each wind speed. Whether the optimum cross-over frequency can be achieved at any particular wind speed depends on the capabilities of the actuator. The objective of the investigations presented in this paper is to design a controller which changes continuously in such a way that the controller is always the most appropriate for the wind speed. Unfortunately, a direct measurement of the wind speed is not possible. Indeed, there is no such thing as "the windspeed" experienced by the wind turbine. Simple scheduling is not appropriate and the wind speed must be inferred from the plant dynamics.

The paper is organised as follows. Section One outlines the controller specifications. In Sections Two and Three a nonlinear controller design is discussed, and in Section Four simulation results are briefly presented comparing this controller with more conventional designs, and some conclusions are reached.

1. Controller Specifications

In order to provide a fair comparison between the various controllers studied, all are designed to meet the following requirements:

- (i) Gain margin of at least 10 dB.
- (ii) Phase margin of approximately 60 degrees.
- (iii) Pitch acceleration standard deviation no more than approximately 45 deg/s².

It is standard practice for wind turbine controllers to include a nonlinear gain to compensate for the variation with wind speed in the sensitivity of aerodynamic torque to pitch change (see e.g. [3]). The representation of the aerodynamics is subject to considerable uncertainty and the gain of the controller is incapable of always being scheduled to match the varying windspeed. Consequently, good gain and phase margins are required to achieve adequate stability margins. If these are not achieved the system must sometimes destabilise, although not necessarily become unstable, when the wind turbine would experience large load fluctuations; that is, the drive-train would resonate. Requirement (iii) represents a practical limitation imposed by the blade servo system. Attention is restricted to continuous-time controller implementations. In previous work by Leithead & Agius [2], the application of linear controllers designed using a classical loop-shaping methodology [3] to a commercial design of two-bladed wind turbine has been investigated. While the controller complexity was severely restricted by limitations in the digital control hardware, and the full potential of the design methodology could therefore not be realised, the generic simulation model used was thoroughly validated for the two-bladed case, and is used in the present work to predict the performance of a nonlinear controller. A linearised version of the full nonlinear wind turbine simulation model was used for control design purposes (figure 2).

2. Nonlinear Controller

The objective is to design a controller whose cross-over frequency varies with wind speed so as to be near optimal, within the limitations allowed by the actuator. In practice, a measurement of wind speed is unavailable, and so the controller is varied on pitch demand instead. If the controller is operating correctly, the demanded pitch angle is a good indicator of wind speed. This approach is in widespread use for varying the nonlinear gain noted in Section One, which is used to compensate for variations in the aerodynamic torque sensitivity. A series of linear controllers is designed for various wind speeds using classical loop-shaping design techniques. Some care was taken to minimise the differences between these controllers so that interpolation between them could be carried out as smoothly as possible. The continuous family of controllers thereby generated is :

$$g = \frac{(s^2+7.59s+68.06)(s+1.7)(s+1.8)(s^2+3s+416.16)}{(s^2+as+b)s(s+0.3)(s+3.75)(s^2+8s+416.16)} \times \frac{(s^2+2s+104.04)(s^2+7.243s+38.637)2209}{(s^2+11s+104.04)(s+100)(s+30)(s^2+65.8s+2209)}$$

where,

$$a = -0.033047p^2 + 0.75064p + 3.3749$$

$$b = 2.6002p + 58.040$$

$$g = (0.13779p + 0.29784) 68.06/b$$

and p is the pitch angle demanded by the controller, in degrees.

The nonlinear controller has the following features :

- Low frequency shaping to improve disturbance rejection.
- Notches at 2P and 4P to reduce actuator activity and prevent the enhancement of the loads induced by these spectral peaks
- High frequency roll-off to reduce actuator activity.

Upper and lower bounds are placed on a, b and g. When p is less than 3.84 degrees (corresponding to 12 m/s rated wind speed), a, b and g are held at their 3.84 degree values. Similarly, when p is greater than 20.59 degrees (24 m/s rated wind speed), a, b and g are held at their 20.59 degree values. It can be seen that these controller transfer functions are the same except for a varying gain and a pair of varying poles. The gain and phase margins of these controllers as p is varied are as follows:

p (deg)	gain margin (dB)	phase margin (deg)	cross-over freq (r/s)
3.84 (12 m/s)	13.74	55.23	1.36
11.14 (16 m/s)	10.03	55.89	2.51
16.21 (20 m/s)	10.00	55.62	2.85
20.59 (24 m/s)	10.79	55.64	3.25

The optimum cross-over frequencies to minimise the standard deviation of the power output are approximately 1.5 r/s, 2.25 r/s, and 4 r/s at 12 m/s, 16 m/s, and 23 m/s respectively for this configuration of wind turbine [1]. While at 24 m/s the optimum cross-over frequency of around 4 r/s is not achieved due to the physical limitations of the actuator, the minima is broad and the cross-over frequency of 3.25 r/s is near optimal.

The gain margin of the 12 m/s controller can be seen to be rather higher than 10 dB. Since there is always a trade-off between performance and robustness, this controller will not achieve the best performance possible at low wind speeds. This choice of controller is necessary, however, if the variation between the transfer functions of the controllers is to be restricted to the values of a, b and g.

The controller is split into two main blocks as shown in figure 3 to cater for the situation when a negative pitch angle is demanded, i.e. when the wind speed has fallen below the level at which rated power of 300 kW can be generated. In this situation the controller is switched out of operation. Due to the presence of low frequency dynamics within the controller, transients may occur for a substantial period of time when the controller is switched back in again as the wind speed rises. To combat this, a minor loop is introduced within the controller, which is activated during below rated operation so that the controller is continuously operating and therefore smooth switching can be ensured. The cross-over frequency of the inner block is chosen to have approximately

the same cross-over frequency as the open-loop transfer function (see [3] for more details). The blocks were chosen as follows:

Inner Block

$$g \cdot 1.813 K_{nl} \frac{(s+1.7)(s+1.8)(s^2+7.59s+68.06)}{s(s+0.3)(s+3.75)(s^2+as+b)}$$

Outer Block

$$1218.484 \frac{(s^2+7.243s+38.637)(s^2+2s+104.04)}{(s+100)(s+30)(s^2+11s+104.04)(s^2+65.8s+2209)} \\ \times \frac{(s^2+3s+416.16)}{(s^2+8s+416.16)}$$

where K_{nl} is the standard nonlinear gain included to compensate for the variation with wind speed in the aerodynamic torque sensitivity to pitch change.

A nonlinear controller is obtained by interpolating continuously between these linear controllers as pitch demand varies. Using the pitch demand to alter the controller introduces additional feedback loops into the system which must be accounted for. The output from the controller now depends on the values of the controller parameters, but these in turn depend on the controller output, which may significantly affect its performance. The outer block of the controller is linear and time-invariant, whilst the inner block contains the nonlinear elements. The effectiveness of such a nonlinear controller depends on the manner in which it is realised. The realisation depicted in figure 4 was determined to be the most appropriate. It causes the achieved performance at any wind speed to match that of the equivalent linear system.

3. Stability Analysis

The stability and robustness of a controller such as the nonlinear one described in the preceding section can be studied using a variety of methods, although the analytical tools available give results which in general are more conservative than in the linear case. Three approaches to stability and robustness analysis are investigated, namely:

- (i) Simulation.
- (ii) Small Gain theorem.
- (iii) Rate of controller variation.

(i) Extensive simulations were carried out with the controller, for various wind conditions. In all cases the controller is observed to exhibit extremely good behaviour, as discussed in the next section. In further simulations, the gain of both the inner and outer blocks of the controller was increased, and a gain margin of around 10.9 dB is observed at wind speeds around 24 m/s. At lower wind speeds the gain margin appears to be greater. This behaviour is in surprisingly good agreement with the gain margins predicted by the linear analysis carried out when designing the

controller. By introducing a first order all-pass network with a non-minimum phase zero, the effect of phase changes was also investigated. In simulations the system appears to be marginally stable for a non-minimum phase zero at $s=-5$, corresponding to a 62 degree phase lag at 3 r/s, the approximate controller cross-over frequency.

(ii) Using the Small Gain theorem (e.g. see [4]), analytic stability results may be obtained with the arrangement in figure 5 (N_0 is a time-invariant approximation to the time-varying second-order network, N ; C_0 is outer block of controller plus time-invariant part of inner block; g_L is a constant gain). In this set-up, for the purpose of calculating the stability margins it is assumed that the variation in the sensitivity of the aerodynamic torque to pitch changes is perfectly compensated for by K_{nl} in the controller. This is clearly unrealistic, and is one of the main reasons that a good gain margin, as calculated assuming perfect compensation, is required for all wind turbine controllers. By varying g_L and using the Small Gain theorem, two bounds on $|g_L + \Delta|$ for stability are found to be (a) (0.00, 5.55) and (b) (3.33, 11.49). The Δ represents the lumped effects the nonlinear behaviour of both the second-order network, N , and the control gain, g , which can be separated as follows. N is obtained by interpolating between linear time-invariant operators N_L . With the 24 m/s case as N_0 , the ratios between the magnitudes of $N_L(s)$ and of $N_0(s)$ are easily be calculated (where N_L' denotes the Laplace transform of N_L , etc). Taking the peak value of these ratios as an estimate of $1 + |\Delta_N|$, bounds on $|\Delta_g|$ are found from those on $|\Delta|$, giving the two ranges (a) (0.00, 5.30) and (b) (3.18, 10.97) for $|\Delta_g|$. The inner block gain of the controller lies in the range (1.50, 3.46). Range (a) for $|\Delta_g|$ indicates that the system should be stable for the nominal plant and controller, while range (b) indicates that the variation in the inner block gain may be increased by a factor of at least 3.17 i.e. there is a gain margin of at least 10.02 dB. While the Small Gain theorem only gives sufficient conditions for stability, the gain margin predicted is in good agreement with that observed in simulations and predicted by linear analysis.

(iii) It is known that if the rate of variation is sufficiently slow, the class of nonlinear system considered here will exhibit the same stability and robustness properties as the sequence of linear time-invariant systems that it interpolates between [5]. In the following analysis it is assumed that the nonlinear second-order network, N meets these requirements i.e. it varies sufficiently slowly, and it is then shown that the controller gain also varies sufficiently slowly for stability to be inferred from a linear analysis. The assumption concerning N can be justified as follows: as noted above, the nonlinear behaviour of N is confined to frequencies above 5 r/s, with constant unity gain at lower frequencies. Linear analysis should therefore certainly apply at low frequencies. Now, N is varied with pitch demand, which has little frequency content above 2-3 r/s. Therefore with respect to frequencies above 5 r/s N appears to be slowly varying, as required.

While the bounds on the permissible rate of variation given in [5] are difficult to apply, given the stated assumption concerning N a simpler result by Desoer and Vidyasagar [4]

regarding stability alone and restricted to a nonlinear gain element may be used. For a linear system with a time-varying feedback gain, this states that the closed-loop system will be stable if,

$$\sup_{t \in [0, \infty)} \int_0^t |H_t(t-\tau)(K(t) - K(\tau))| d\tau < 1$$

where, H_t is the impulse response of the stable closed-loop system when the gain is fixed at $K(t)$; that is, $K(\cdot)$ should remain substantially constant during the 'memory time' of $H_t(\cdot)$ (when it differs appreciably from zero). If the maximum magnitude of the rate of change of $K(\cdot)$ is α , then we have that,

$$|K(\tau) - K(t)| \leq \alpha |\tau - t|$$

Numerically evaluating the integral reveals that values of α up to 1.12 are permissible. An estimate of the actual value of α can be obtained as follows :

$$\alpha = dK/dt = (dK/du) (du/dt)$$

where u is the pitch demand signal used to vary the controller.

It is known that $dK/du \leq 0.14$, and from simulations $du/dt \leq 2$ deg/s, so that $dK/dt \leq 0.28$ and the system is stable. Further this result suggests that the nonlinear behaviour is in fact sufficiently slow that stability may be predicted by linear analysis, which is borne out by the results obtained both by simulation and with the Small Gain theorem. Given the rapid variation in pitch demand, the full controller range could be covered in a few seconds, this is a somewhat unexpected conclusion.

While none of the stability results that have been presented are conclusive, it is believed that they are based on reasonable assumptions and they appear to be consistent with one another and in agreement with the behaviour observed in simulations.

4. Controller Performance

The performance of the nonlinear controller was investigated using a well validated simulation model. It is compared with the performance of conventional controllers designed to meet the same specifications. These controllers are as follows.

PI Controller $0.961 \times 10^{-3}(1+10.504/s)$
(gain margin 10 dB, phase margin 76.14 degrees, cross-over frequency 1.58 r/s)

Linear Classical Controller (see e.g. [2,3]):

$$871.229 \frac{(s+1.6)^2(s^2+7.243s+38.637)}{s(s+0.3)(s+3.7)(s+20)(s+50)}$$

$$\frac{(s^2+1.5s+104.04)(s^2+6s+416.16)}{(s^2+11s+104.04)(s^2+10s+416.16)(s^2+65.8s+2209)}$$

(gain margin 10 dB, phase margin 56.14 degrees, cross-over frequency 1.826 r/s)

This is similar to previous classical controllers used with a commercial two-bladed design of wind turbine [2].

Simulations were run with these controllers over a range of wind speeds and turbulence levels to reproduce the real machine conditions noted in [2], and to predict performance at higher wind speeds. Four mean wind speeds of 12, 16, 20 and 24 m/s were used at three nominal turbulence levels of 10, 15 and 20 %. The simulations were run for 260 seconds, giving four one minute periods of data. The nominal turbulence level only applies over a long time period, and the range of turbulence levels for the 1 minute samples was 6 - 26 %. These runs produced only 48 data points to cover the whole operational range of the machine, but this approach has nevertheless been found to be a good indicator of the comparative performance between controllers [2].

Probability distributions of the power time histories for these controllers are given in figure 6 at a mean wind speed of 24 m/s and 10% and 20% turbulence intensity. A large reduction in the time spent at high power levels is evident with the nonlinear controller. For example, the percentage of time that the power level exceeds 400 kW for the various controllers is as follows.

	10% Turbulence	20% Turbulence
PI	5.53%	18.82%
linear classical	2.09%	14.04%
nonlinear	0.58%	5.09%

For comparison, the percentage of time exceeding 450 kW at 20% turbulence is as follows.

PI	8.60%
linear classical	4.02%
nonlinear	0.64%

Linear fits are made to the power maxima from the 1 minute samples with turbulence in the range 8-18% , corresponding to the wind regime experienced in [2], and also to samples with turbulence in the range 13-26%, corresponding to a slightly more severe situation. The equations of these fits are as follows.

Turbulence	Controller	Fit	Standard Deviation
8-18%	PI	$7.65 * \text{wind} + 288.82$	18.96
	classical	$6.86 * \text{wind} + 296.44$	19.99
	nonlinear	$4.71 * \text{wind} + 326.01$	11.78
13-26%	PI	$11.67 * \text{wind} + 240.37$	29.02
	classical	$8.49 * \text{wind} + 280.05$	20.02
	nonlinear	$5.11 * \text{wind} + 330.49$	14.52

The PI controller's maxima increase at the fastest rate, followed by the linear classical controller and finally the nonlinear controller, which has around half the rate of

increase of the PI controller, and much lower standard deviations, corresponding to a tighter bunching of the maximums.

The pitch acceleration standard deviations for the 1 minute samples with turbulence in the range 8-18% are shown in figure 7. The PI controller works the actuator least, and has the lowest standard deviation, while the conventional classical controller has a slightly higher level of activity. The standard deviation in both these cases falls as the wind speed rises, due to the increase in the sensitivity of the aerodynamic torque to pitch changes. In contrast, the standard deviation for the nonlinear controller remains roughly constant as wind speed rises, exploiting the extra actuator capacity available at higher wind speed, as intended.

5. Conclusions

To conclude, a nonlinear controller has been designed which changes continuously in such a way that the controller is always the most appropriate for the wind speed, even though a direct measurement of wind speed is not possible but must be inferred. This controller is found to have the desired stability robustness, as far as can be determined. In extensive simulations using a well validated model, it is found to give significant performance improvements over both PI and a linear classical controllers. In particular, both the peak power, and the time spent at high power levels are greatly reduced, with a consequent reduction in drive-train loads. This improvement is obtained by exploiting the actuator capability that is left unused at higher wind speeds by linear time-invariant controllers.

Acknowledgements

The SERC, DTI (formerly D.En) and ETSU are gratefully acknowledged for supporting the work presented here, and by whose permission this paper is published.

References

1. Leithead, W.E., Rogers, M.C.M., 1993, 'A Comparison of the Performance of Constant Speed HAWT's', presented at 'Renewable Energy - Clean Power 2001', Nov. 1993, London, IEE Conference Publication No. 385.
2. Leithead, W.E., Agius, P.R.D., 1991, 'Application of Classical Control to the WEG MS3 Wind Turbine', Industrial Control Centre, Report 342, University of Strathclyde.
3. Leithead, W.E., de la Salle, S.A., Reardon, D.L., Grimble, M.J., 1991, 'Wind Turbine Control Systems Modelling and Design Phase I and II, DTI Report No. ETSU WN 5108.
4. Desoer, C.A., Vidyasagar, M., 1975, Feedback Systems: Input-Output Properties', Academic Press, London.
5. Shamma, J.S., Athans, M., 1990, 'Analysis of Gain Scheduled Control for Nonlinear Plants', IEEE Trans Aut Control, Vol. AC-35, pp898-907

Figure 1 typical wind spectrum for two-bladed machine

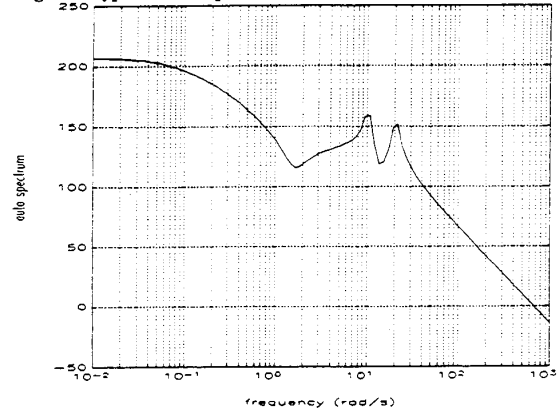


Figure 2 Linearised control model

Rotor Radius: 16.5m Grid Frequency: 50 Hz
 Generator Slip: 2% Rotor Speed: 5.02 rad/s
 First Drive-Train Mode: 6.216 r/s, damp 0.583
 (corresponds approximately to configuration 3 in [1])
 dQ/dp is sensitivity of aerodynamic torque to pitch changes.
 dQ/dV is sensitivity of aerodynamic torque to wind speed.

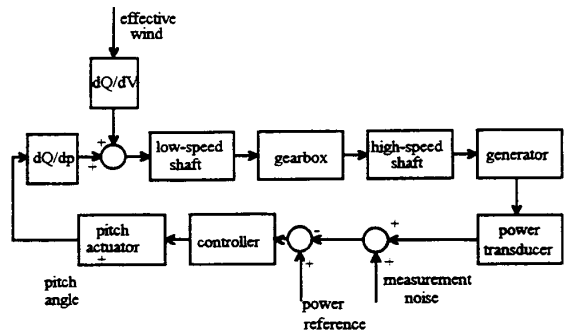


Figure 3 Controller structure

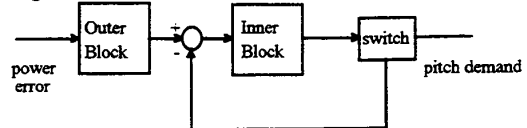


Figure 4 Realisation of inner block of nonlinear controller

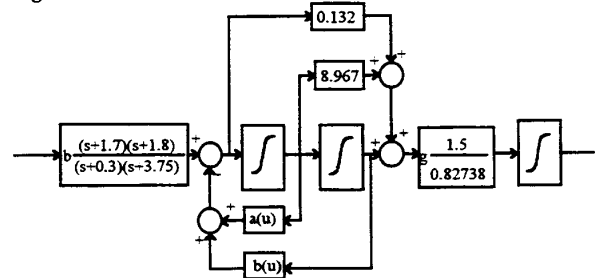


Figure 5 Arrangement used with Small Gain Theorem analysis

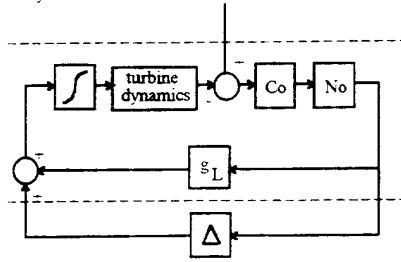


Figure 6a Probability distribution of power, 24 m/s, 10% TI

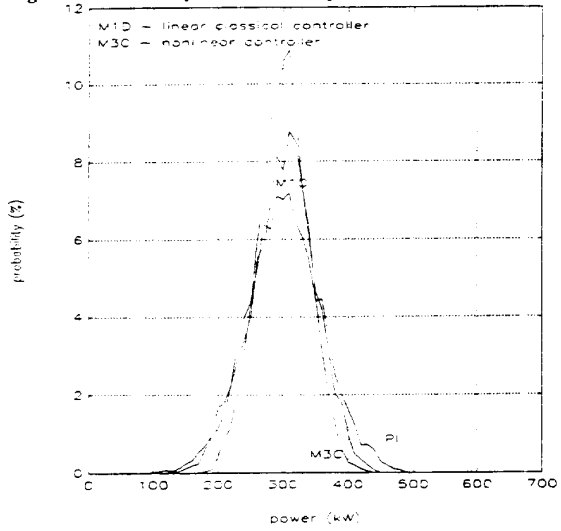


Figure 6b Probability distribution of power, 24 m/s 20% TI

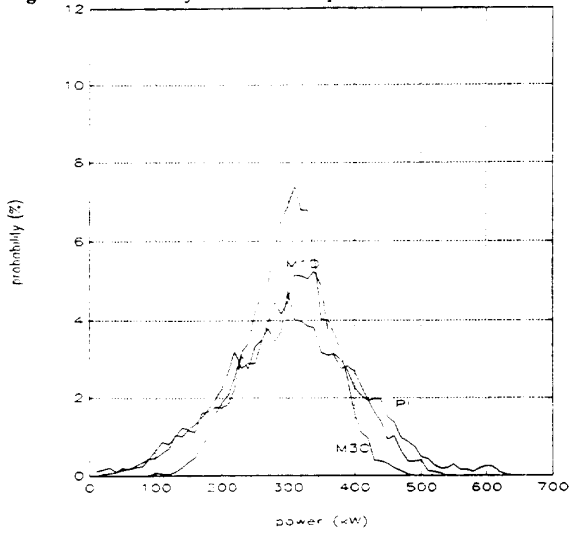


Figure 7 Pitch acceleration standard deviation + PI
 • linear classical controller
 x nonlinear controller

